

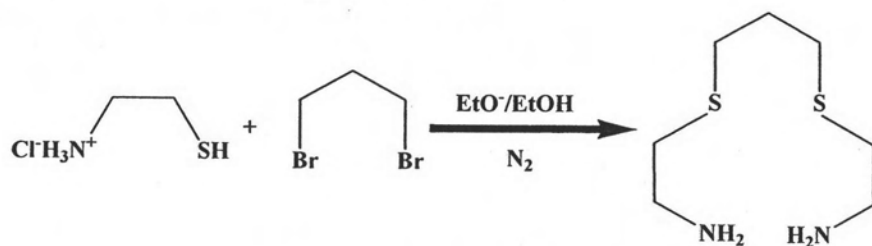
CHAPTER IV

RESULTS AND DISCUSSIONS

4.1 Characterization

4.1.1 Characterization of chelating ligand AEPE

The chelating ligand AEPE, used to modify the hectorite clay, was synthesized by using the method proposed by Choudhury and coworkers (1991) [41] (Scheme 4.1). The reaction between cysteamine hydrochloride and 1,3-dibromopropane occurred via nucleophilic substitution reaction. The nucleophile, produced by abstraction of a proton of $-SH$ groups by ethoxide base, reacted with 1,3-dibromopropane which had bromide as leaving groups. The synthesis of AEPE was carried out with the mole ratio of cysteamine hydrochloride:1,3-dibromopropane equal to 2:1. The final product was obtained as yellow oil with 79% yield of AEPE.



Scheme 4.1 Synthesis of AEPE.

4.1.1.1 Nuclear magnetic resonance spectroscopy

The $^1\text{H-NMR}$ spectrum of AEPE was recorded in CDCl_3 (Figure 4.1). It shows 3 positions of aliphatic proton region due to symmetrical structure of AEPE as follow:

δ (ppm) 1.77 (t, 2H, $J = 7.02$ Hz), 2.53 (t, 8H, $J = 6.24$ Hz) and 2.78 (t, 4H, $J = 6.24$ Hz). The ^{13}C -NMR spectrum of AEPE was obtained with chemical shifts as follow: δ (ppm) 29.40 (s, 1C), 30.46 (s, 2C), 36.18 (s, 2C) and 41.02 (s, 2C) as presented in Figure 4.2. These results indicate that AEPE was successfully synthesized.

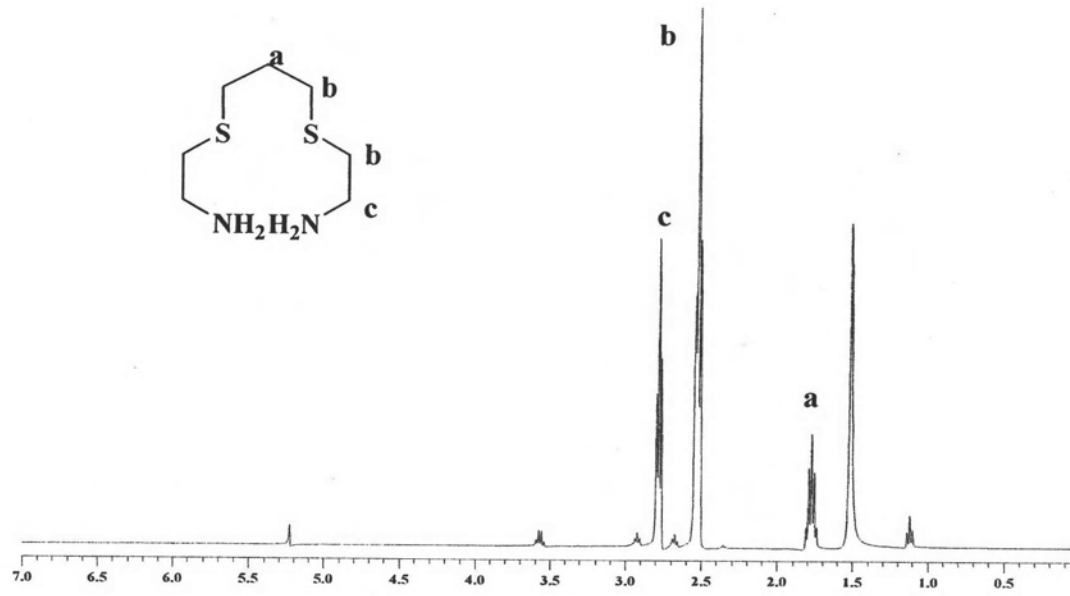


Figure 4.1 ^1H -NMR spectrum of AEPE in CDCl_3 .

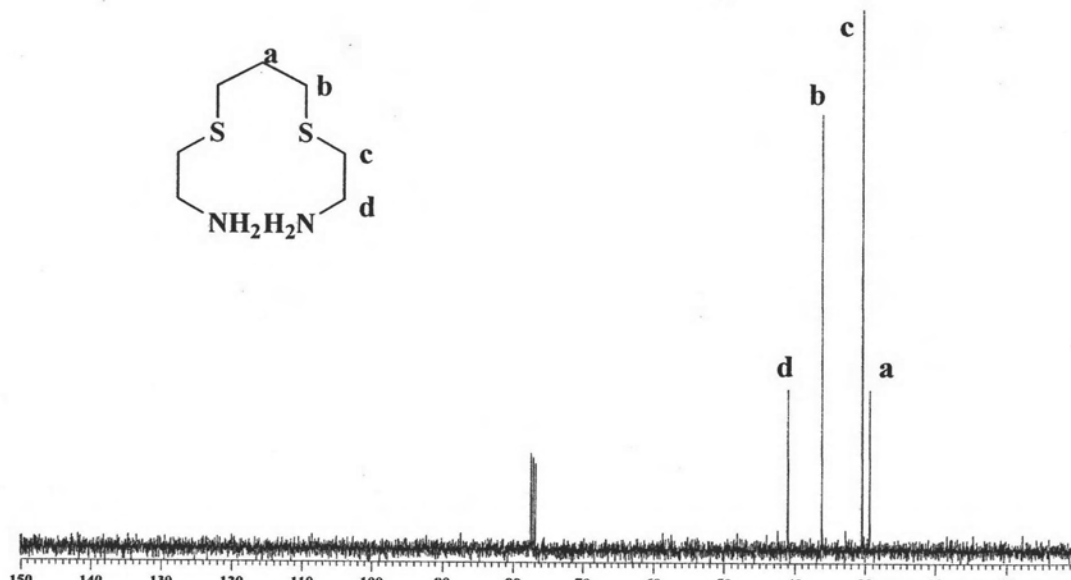
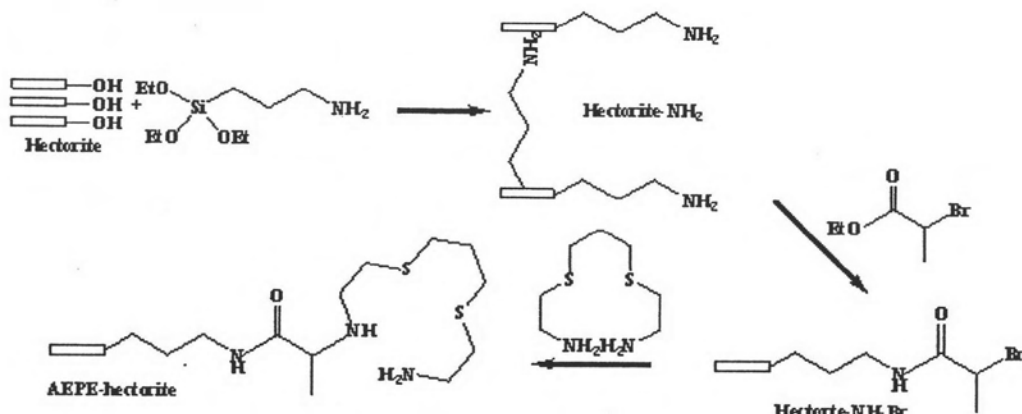


Figure 4.2 ^{13}C -NMR spectrum of AEPE in CDCl_3 .

4.1.2 Characterization of modified hectorite

The functionalization of hectorite with AEPE (Scheme 4.2) started with silanization of 3-aminopropyltriethoxysilane onto the surface of hectorite. The reaction occurred between ethoxy groups and hydroxyl groups (act as nucleophile) on surface to obtain the hectorite-NH₂ product. In the second step, amino groups of hectorite-NH₂ reacted with ethyl-2-bromopropionate via nucleophilic substitution reaction to form amide bond in the product (hectorite-NH-Br). In the last step, the final product (AEPE-hectorite) was obtained by nucleophilic substitution of hectorite-NH-Br by amino groups of AEPE ligand. All processes were performed under nitrogen atmosphere, using reflux temperature of 80-100°C.



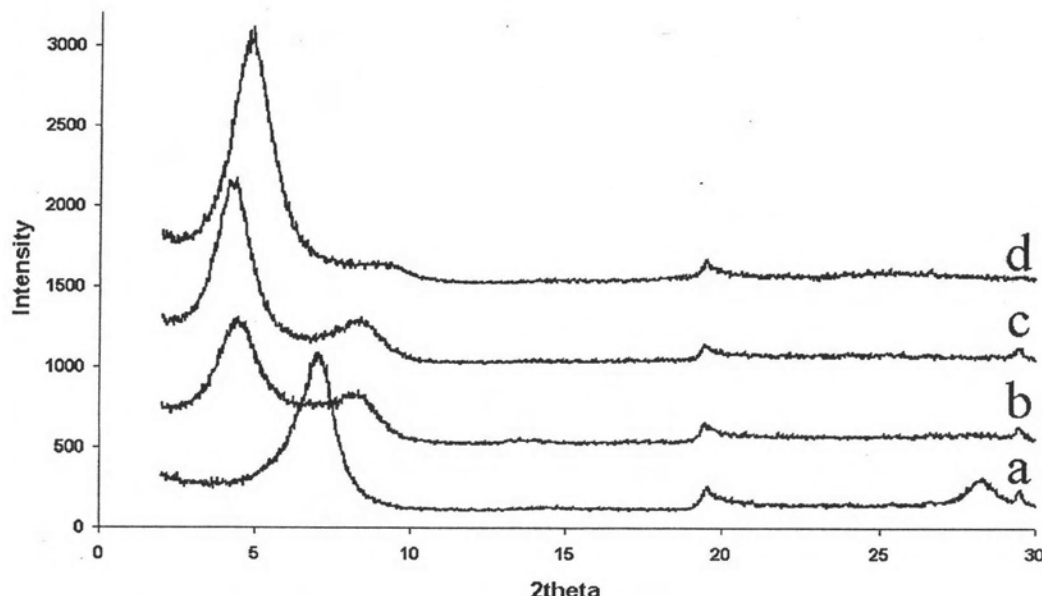
Scheme 4.2 Modification of hectorite with AEPE.

4.1.2.1 X-ray diffraction spectroscopy

X-ray diffraction spectroscopy was used to characterize the structure of unmodified and modified hectorite. The results are presented in Table 4.1 and Figure 4.3.

Table 4.1 The basal spacing (d_{001}) of unmodified and modified hectorite

Sample	d_{001} (Å)	2θ (°)
Hectorite	12.7	6.9
Hectorite-NH ₂	20.0	4.4
Hectorite-NH-Br	21.1	4.1
AEPE-hectorite	18.4	4.8

**Figure 4.3** XRD patterns of hectorite (a), hectorite -NH₂ (b), hectorite-NH-Br (c) and AEPE-hectorite (d).

The XRD pattern of hectorite (Figure 4.3a) showed characteristic peaks at 6.9°, 19.6° and 28.2° 2θ indicating that hectorite have the crystalline structure of silicate clays of the type 2:1 (T:O:T) layer silicate [1, 11]. Moreover, the peak at 19.6° 2θ was also observed in the XRD pattern of AEPE-hectorite (Figure 4.3d) indicating that the original structure of hectorite was preserved after functionalization.

In order to investigate the modification within hectorite interlayer spaces, change of d_{001} spacing was followed for all products and summarized in Table 4.1. The basal spacing of hectorite-NH₂ increased to 20.0 Å (Figure 4.3b) from 12.7 Å spacing

of hectorite (Figure 4.3a) due to the intercalation and subsequent grafting of 3-aminopropyltriethoxysilane. The grafting [11] was expected via the condensation of ethoxy groups of (3-aminopropyl)-triethoxysilane and protons (SiO-H) on clay surface. In the second step, ethyl-2-bromopropionate was added and an insignificant change of d_{001} spacing of hectorite-NH-Br (Figure 4.3c) was observed. This result may be explained as the intercalation of smaller molecules of ethyl-2-bromopropionate did not increase the clay gallery height. The existence of ethyl-2-bromopropionate will be confirmed in a later section. The addition of AEPE lowered the basal spacing to 18.4 Å (Figure 4.3d). This result could be explained that the AEPE molecules intercalated into the empty space between the pre-expanded layers of hectorite-NH-Br and subsequently grafted. With the presence of thioether group in the ligand, the van der Waals interaction among ligand chains may be expected, leading to its structural rearrangement and the contraction of the gallery height. In conclusion, the synthesis of AEPE-hectorite was successful and AEPE could be grafted on both the external and interlayer surface of hectorite.

4.1.2.2 Fourier transforms infrared spectroscopy

The functional groups of unmodified and organic modified hectorite were studied by FT-IR and FT-IR spectra of hectorite, hectorite-NH₂, hectorite-NH-Br and AEPE-hectorite are displayed in Figure 4.4. The assignments for the FT-IR bands of the unmodified clay and the new bands occurring after modification with organic agents are listed in Table 4.2.

Table 4.2 FT-IR vibration band position and their assignments for unmodified and modified hectorite [43-48]

	Band position (cm ⁻¹)	Assignments
Original band ^a		
	3678	$\nu_{\text{Mg-OH-Mg}}$ (multiple bands)
	3629	$\nu_{\text{Mg-OH-Mg}}$ (structural effects)
		$\nu_{\text{w(1)}}$, high frequency vibration, weak
		H-bonds, remaining H ₂ O coordinated on
		cations in dehydrated sheet structure
		silicates
	3436	ν_{w} , H ₂ O
	2350	CO ₂ stretching vibration
	1634	$\nu_{\text{w(1)}}$, liquid alike water with strong intramolecular H-bonds
	1001	$\nu_{\text{Si-O}}$, tetrahedral Si-O vibration
	881	$\delta_{\text{Al-OH}}$, octahedral Al-OH
	802	$\delta_{\text{Al-Mg-OH}}$, octahedral Al-Mg-OH
	649	$\delta_{\text{Mg-OH}}$, octahedral Mg-OH
	463	$\delta_{\text{Si-O}}$, Si-O-Si vibration

Table 4.2 FT-IR vibration band position and their assignments for unmodified and modified hectorite (continued)

	Band position (cm ⁻¹)	Assignments
New band ^b	2925-2935	$\nu_{\text{C-H}}$ stretching vibration of aliphatic C-H
	1724-1730	$\nu_{\text{C=O}}$ stretching vibration
	3262	ν_{NH_2} stretching vibration

(ν = stretching vibrations, δ = bending vibrations)

^a Hectorite

^b Modified hectorite (hectorite -NH₂, hectorite-NH-Br and AEPE-hectorite)

The new bands that appeared at 2933, 2930 and 2927 cm⁻¹ in the spectra of modified hectorite (Figure 4.4 b-d), belong to an aliphatic C-H stretching vibration. Furthermore, IR spectra of hectorite-NH-Br (Figure 4.4c) and AEPE-hectorite (Figure 4.4d) show C=O stretching at 1725 cm⁻¹ and N-H stretching of amine at 3262 cm⁻¹, respectively. These results confirm the functionalization of the clays with ethyl-2-bromopropionate and AEPE ligand, respectively. Moreover, IR bands at about 3678, 650, 1001 and 460 cm⁻¹ that are characteristic bands of a natural hectorite [43] were also observed in the spectra of modified hectorites, indicating that the original structure of hectorite was preserved after modification.

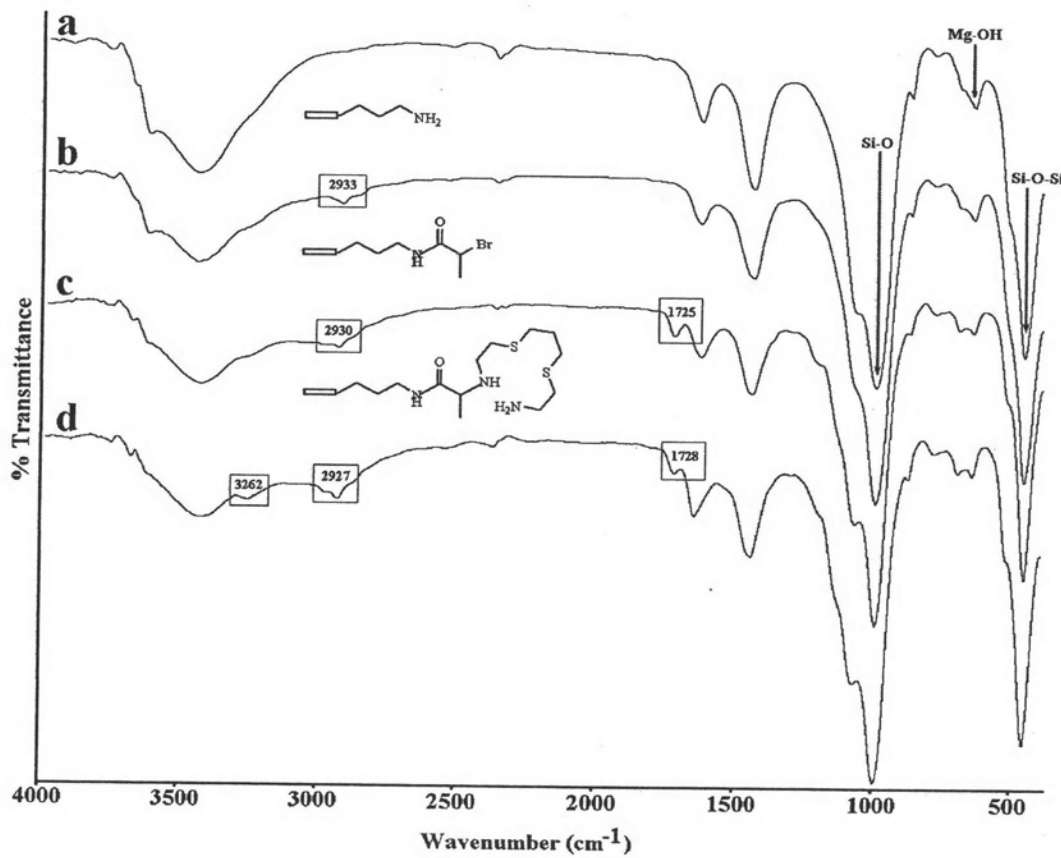


Figure 4.4 FT-IR spectra of hectorite (a), hectorite -NH₂ (b), hectorite-NH-Br (c) and AEPE-hectorite (d).

4.1.2.3 Thermo gravimetric analysis

The thermal stability of the modified products was investigated to confirm the success of modification of hectorite with organic agents. The results from thermogravimetric analysis (TGA) are presented in Figure 4.5. The TGA curves of the unmodified and modified hectorites show the weight loss at temperature below 200°C and above 600°C due to the vaporization of moisture and/or organic solvents [23, 49] and the dehydroxylation of aluminosilicate groups [36, 49-50], respectively. Furthermore, the decomposition of the organic compounds on the modified clays was

observed from the weight loss in the temperature range of 200-550°C as shown in Figure 4.5b-d.

The TGA curve of hectorite-NH₂ (Figure 4.5b) shows a weight loss of 4.54 % at the temperature range of 300-550°C. This loss of weight corresponds to the loss of aminopropyl groups added to hectorite surface in the first step. In addition, the significant increase in weight loss above 550°C of hectorite-NH₂ compared to hectorite confirms that the siloxy groups from 3-aminopropyltriethoxysilane were present and that 3-aminopropyltriethoxysilane was grafted on the hectorite surface. An increase in weight loss in the range of 200-550°C was observed when hectorite-NH₂ was modified with ethyl-2-bromopropionate and AEPE ligand, respectively (Figure 4.5c-d). These results indicate the difference of chemical composition on the hectorite surface and confirm the success of modification.

4.1.2.4 Elemental analysis

The result of elemental analysis can be used to explain the modification of hectorite by observing the change of the percentage of C, H and N of the obtained products as presented in Table 4.3. An increasing of C, H and N (wt %) was observed in hectorite-NH₂ and AEPE-hectorite, respectively, compared to those in hectorite. More importantly, the presence of percentage nitrogen observed only in hectorite-NH₂ and AEPE-hectorite ensures the modification of hectorite with 3-aminopropyltriethoxysilane and AEPE, respectively. Moreover, the theoretical values of C, H and N (wt %) were calculated by using the organic part of one unit of AEPE-hectorite for comparison. It was seen that the theoretical values are clearly higher than the experiment values because the experiment values were calculated using the weight of the whole AEPE-hectorite. However, the C/N ratio of AEPE-hectorite was close to the theoretical C/N ratio. This result reveals that hectorite was modified with the desired ligand.

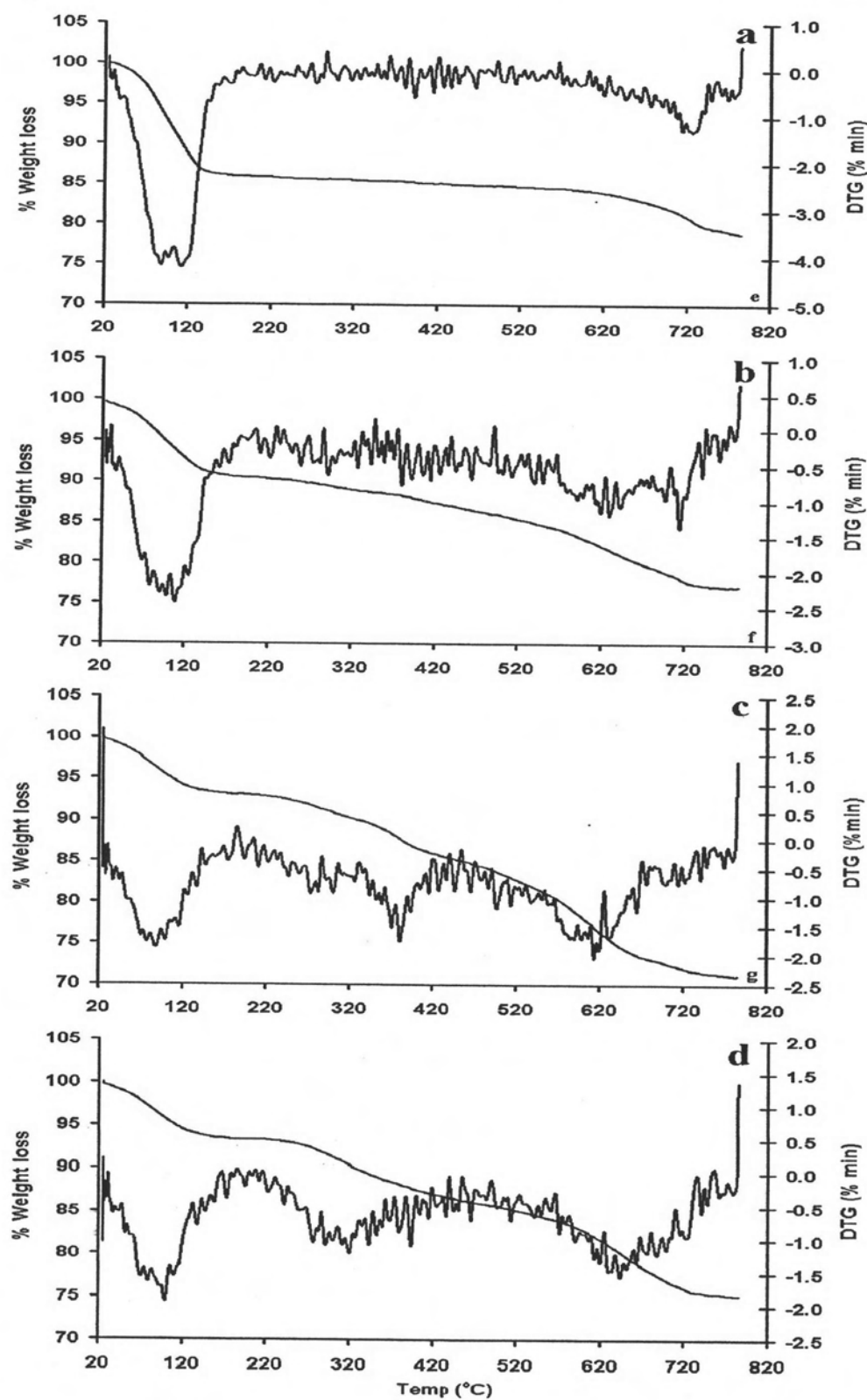


Figure 4.5 TGA-DTG curves of hectorite (a), hectorite -NH₂ (b), hectorite-NH-Br (c) and AEPE-hectorite (d).

4.1.2.5 Surface area analysis

Finally, the surface area of hectorite and AEPE-hectorite were determined and the results are shown in Table 4.3. The results show a significant decrease of surface area in AEPE-hectorite compared to hectorite due to the coverage of the pores and interlamellar sites with AEPE molecules. These results confirm the presence of organic molecules on the surface of hectorite

Table 4.3 CHN analysis and surface area of the unmodified and modified hectorite

Phase	Elemental analysis			C/N ratio	Surface area (m ² g ⁻¹) ^a
	C	H	N		
Hectorite	1.37	0.48	n.d. ^b	-	54.48
Hectorite-NH ₂	4.37	1.75	0.65	-	-
AEPE-hectorite	9.63	2.16	1.78	5.30	16.48
Theoretical ^c	50.95	9.14	13.72	4.34	-

^a Determined by surface area analysis (N₂ adsorption and BET method)

^b n.d. = not detectable

^c Calculated from one unit of AEPE-hectorite in the organic part presented in scheme 4.2.

The results from XRD, FT-IR, TGA, EA and surface area analysis confirm the successful modification of hectorite with the chelating ligand AEPE. The modified hectorite was further used in the adsorption of Hg(II) and Ag(I) ions in aqueous solutions.

4.2 Adsorption study using batch method

The hectorite successfully modified with AEPE was used in adsorption study of Hg(II) and Ag(I) ions in aqueous solutions using batch method. The effect of various parameters such as pH of metal ions solutions, extraction time, adsorbent dose, ionic strength, interfering ions were investigated to obtain the suitable conditions for metal ions extraction. The adsorption isotherms were also studied.

The metal adsorption efficiency is presented in term of percentage removal and sorption capacity, calculated according to equation 4.1 and 4.2, respectively.

$$\text{Removal (\%)} = \frac{C_i - C_e}{C_e} \times 100 \quad (4.1)$$

$$\text{Sorption capacity (} q \text{)} = \frac{\frac{C_i - C_e}{1000} \times V_s}{m} \quad (4.2)$$

where C_i = initial concentration of metal ions in aqueous solution
 (mg L^{-1})

C_e = equilibrium concentration of metal ions in aqueous solution
 (mg L^{-1})

q = sorption capacity (mg g^{-1})

V_s = volume of metal ions aqueous solution (mL)

m = weight of adsorbent (g)

4.2.1 Effect of pH of metal ions solutions

The pH of solution is one of parameters that have strong influence on metal adsorption due to the presence of different species of metals at different pH (i.e. metal ions and/or metal hydroxide precipitate) and the protonation or deprotonation of active

sites of ligand (e.g. sulfur and nitrogen donor atoms) that will affect the binding ability with metal species. These could have an impact on removal efficiency of the adsorbents. Therefore, the effect of pH must be studied to gain the suitable pH for metal ion extraction.

The initial pH of Hg(II) and Ag(I) solutions used in this study were in the range of pH 1.0-8.0. It was observed that at the initial pH about 3.0 and higher, the pH at equilibrium increased to 6.0-7.8. This behaviour was observed when used both hectorite and AEPE-hectorite and could be possibly explained by basic properties of hectorite and the ligand (AEPE).

The results of extraction of Hg(II) and Ag(I) in aqueous solutions by unmodified and AEPE-hectorites are shown in Figure 4.6-4.7. It was found that the removal efficiency of AEPE-hectorite was clearly greater than that of unmodified hectorite. The results could be explained by the presence of sulfur and nitrogen donor atoms in AEPE-hectorite which can complex with Hg(II) and Ag(I) ions by the coordination. In addition, regarding to Pearson rule, sulfur donor atom is soft base that can form coordination bond well with soft acids, that are Hg(II) and Ag(I) species in this case [30, 51]. The results show that the extraction efficiencies of Hg(II) in aqueous solutions by unmodified hectorite were very low ($\leq 16.8\%$) at every pH values as shown in Figure 4.6. Regarding the pH of point of zero charge or isoelectric point (pH_{PZC} or iep) [77], that is the pH at which the net surface charge is zero (positive charge equal to negative charge) [12, 32], the pH_{PZC} of smectite (e.g. hectorite, montmorillonite, beidellite and saponite) was reported to be in the range of 6.0-8.0 [11, 52]. If the pH of solution is below pH_{PZC} , the surface of hectorite can be protonated, resulting in positively charged surface, and at the pH above pH_{PZC} , the surface of hectorite can be deprotonated, giving negatively charged surface [29]. Furthermore, the perusal of the literature on Hg(II) speciation diagram [27] shows that Hg(II) species appear as Hg^{2+} and $Hg(OH)^+$ at equilibrium pH below 4.0 and the dominant Hg(II) species at equilibrium pH higher than 4.0 is $Hg(OH)_2$. Therefore, the adsorption of

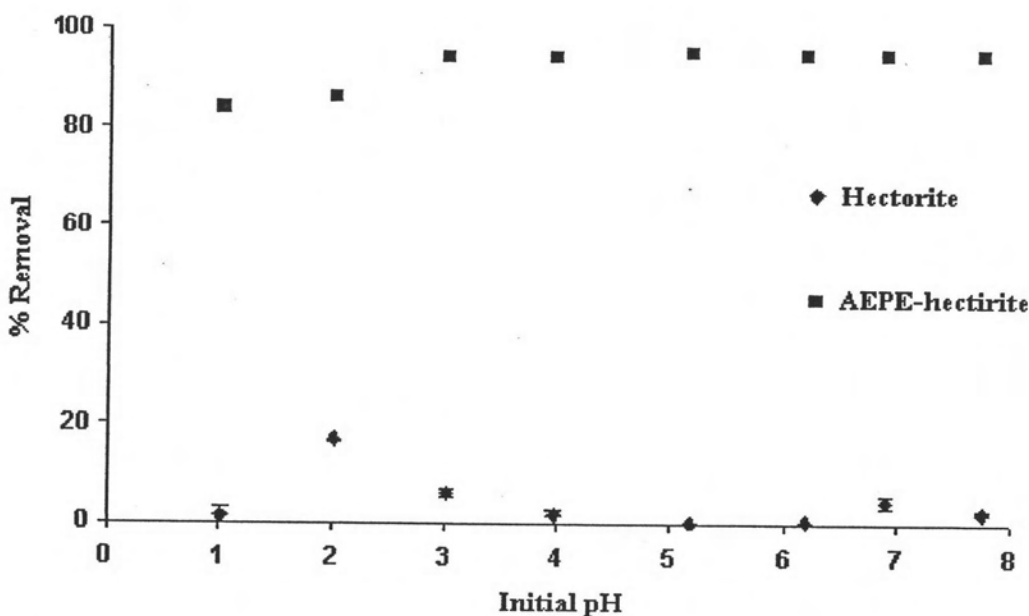


Figure 4.6 Effect of pH on the adsorption of the Hg(II) ions (50 mg L^{-1}) by hectorite and AEPE-hectorite.

Hg(II) at very low pH was not favorable due to electrostatic repulsion between the positively charged surface and metal cations. At equilibrium pH higher than 4.0, the adsorption of the neutral species, Hg(OH)_2 on the charged surface was less likely to occur via electrostatic interaction, resulting in low extraction efficiency. In the case of AEPE-hectorite, it can be seen that the removal percentages increased with increasing the pH of the solutions and attained the optimal value at the initial pH of 3.0-8.0 with the removal efficiency of 95%. It can be explained by the different affinity of the electron donor atoms (sulfur and nitrogen atoms) in the AEPE towards different Hg(II) species, according to the Pearson rule. Neutral molecules are softer acids than metal cations, therefore, the coordination of Hg(II) species at equilibrium pH 4.0-8.0 (Hg(OH)_2) with the AEPE would be highly favorable [2, 30, 51]. On the other hand, at the initial pH of 1.0-2.0, the amine group on the AEPE molecule could be protonated and because of this, the binding ability of the protonated ligand with Hg(II) cations was lower than that of the non-protonated ligand with Hg(OH)_2 at equilibrium pH

values higher than four. As a result, the removal efficiency decreased slightly at equilibrium pH 1.0 and 2.0.

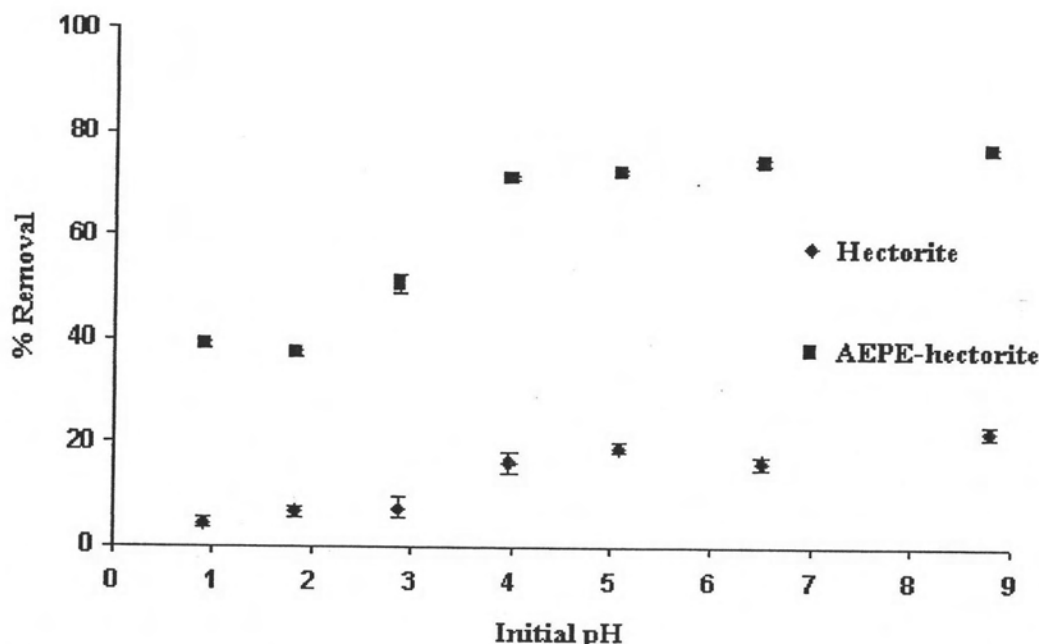


Figure 4.7 Effect of pH on the adsorption of Ag(I) ions (40 mg L^{-1}) by hectorite and AEPE-hectorite.

Figure 4.7 shows the effect of pH on the adsorption of Ag(I) in aqueous solutions by hectorite and AEPE-hectorite. It was observed that the removal percentage of both hectorite and AEPE-hectorite increased in increasing the pH of solution and reached a plateau of maximum value at the initial pH of 4.0-8.0. The maximum values of the removal efficiency were 18.4 and 73.6 % for hectorite and AEPE-hectorite, respectively. The surface of the adsorbents in the solution at this pH range could be negatively charged (equilibrium pH $> \text{pH}_{\text{PZC}}$), while the species of silver in the solutions ($\text{pH} = 2.0-10.0$) was Ag^+ cations [14]. Thus, the adsorption of Ag^+ cations on the surface of adsorbents via electrostatic attraction was favorable when increased the pH of solution from pH 1 to pH 4 and higher. In addition, the active sites of AEPE, e.g. the sulfur and nitrogen donor atoms, enhanced the adsorption efficiency

of AEPE-hectorite by coordination with Ag^+ according to the Pearson rule. On the other hand, when the pH of solution was very low (pH 1.0-3.0), the removal percentages decreased for both modified and unmodified adsorbents. These results could be explained by the protonation of the hectorite surface and the amine group on the AEPE, resulting in positively charged surface and ligand which had low binding ability towards Ag^+ cations.

In conclusion, the suitable pH for extraction are the initial pH of 4.0 and 5.0 (without buffer) for Hg(II) and Ag(I), respectively or the equilibrium pH of 7.0 for both metal ions. In addition, the adsorption equilibrium and the maximum adsorption of Hg(II) and Ag(I) in aqueous solutions by AEPE-hectorite will be discussed later in the section of kinetics and adsorption isotherms.

4.2.2 Effect of extraction time

The adsorption mechanism, which can take place between liquid (solute) and solid (adsorbent) phase, have three main steps as following: (i) bulk transport, (ii) film transport and (iii) intraparticle transport. The bulk transport usually occurs rapidly and therefore, the process of film and/or intraparticle transport is often the rate determining step for adsorption equilibrium. In this experiment, the effect of extraction time was investigated to obtain the equilibrium time for the adsorption process used.

Figure 4.8 shows the adsorption efficiencies of Hg(II) and Ag(I) in solutions by the AEPE-hectorite when using contact times of 1 to 120 min and the initial pH of 4.0 and 5.0 for Hg(II) and Ag(I) solutions, respectively. The results indicate that the adsorption efficiencies increased with the increasing of contact time and reached the equilibrium after 30 and 40 min for Hg (II) and Ag(I), respectively. Therefore, the extraction time of 60 min was chosen for the extraction experiments of both metals to assure the adsorption equilibrium.

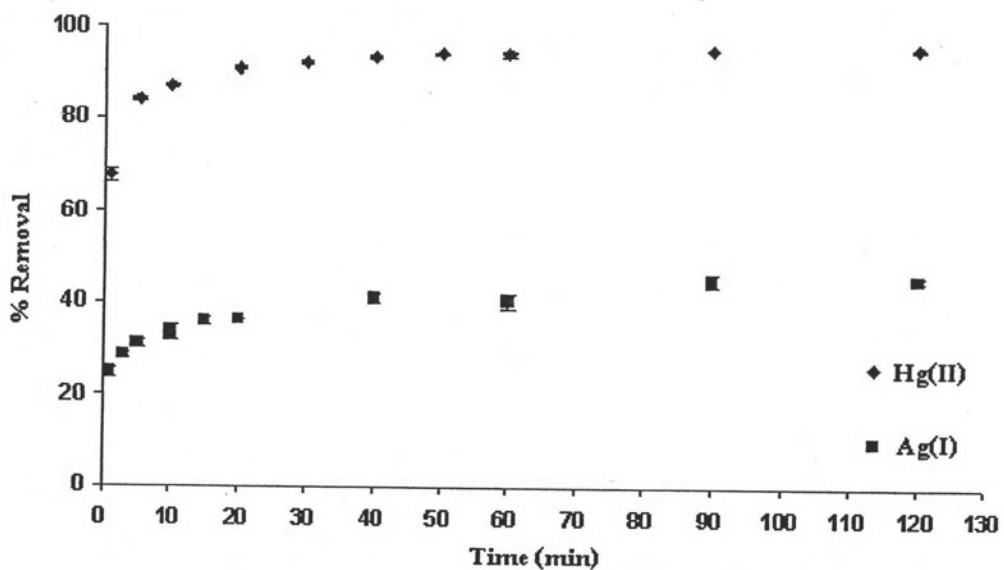


Figure 4.8 Effect of extraction time on the adsorption of Hg(II) and Ag(I) ions by AEPE-hectorite (initial concentration of 50 mg L^{-1} for Hg(II) and 70 mg L^{-1} for Ag(I)).

4.2.3 Adsorption kinetics and effect of adsorbent dose

The effect of adsorbent dose was studied in order to observe the adsorption behavior of AEPE-hectorite by varying the amounts of the sorbents in the range of 0.01 to 0.05 g in the adsorption experiments using 5 mL of Hg(II) (100 mg L^{-1}) and Ag(I) solution (200 mg L^{-1}). In addition, for each adsorbent dose, the contact time was also varied in the range of 1-120 min. The output data were fit to kinetic models for the adsorption.

The results show that the removal percentages were enhanced and the faster equilibrium time was achieved when increased the amount of the adsorbents as shown in Figure 4.9-4.10. It could be explained by an increase in number of the active sites. On the other hand, the adsorption capacity, which is the amount of metal ions sorbed per unit mass of adsorbent, decreased when increased the adsorbent dose. This is mainly due to the unsaturation of active sites at higher adsorbent dose for the same initial concentration [53, 54].

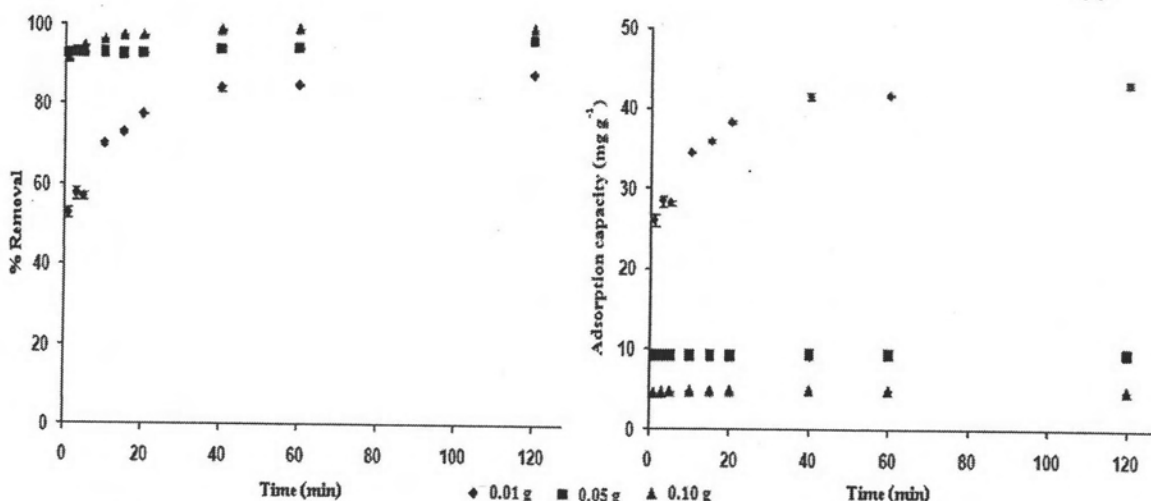


Figure 4.9 Effect of adsorbent dose at the various extraction time on the adsorption of Hg(II) ions by AEPE-hectorite (initial concentration : 100 mg L⁻¹).

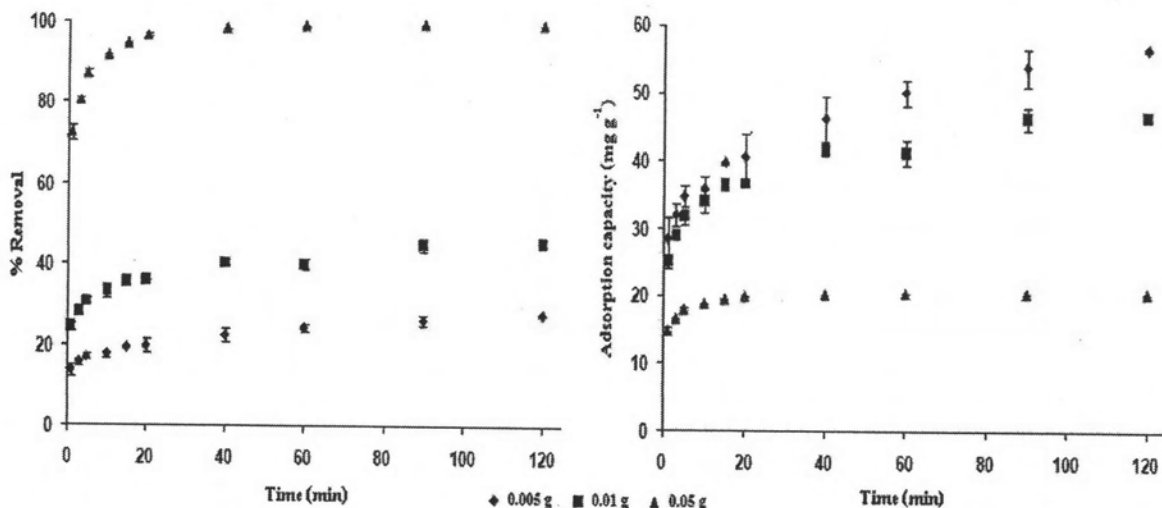


Figure 4.10 Effect of adsorbent dose at the various extraction times on the adsorption of Ag(I) ions by AEPE-hectorite (initial concentration : 200 mg L⁻¹).

In order to investigate the sorption kinetics of Hg(II) and Ag(I) on AEPE-hectorite phase, the pseudo-first order [55] and the pseudo-second order models [79] were applied and the equations of these two models are expressed as equation 4.3 and 4.4, respectively.

$$\log (q_e - q_t) = \log q_e - \frac{k_1}{2.303} t \quad (4.3)$$

$$\frac{t}{q_t} = \frac{1}{k_2 q_e^2} + \frac{t}{q_e} \quad (4.4)$$

where q_e = sorption capacity at equilibrium (mg g^{-1})

q_t = sorption capacity at time (mg g^{-1})

t = extraction time (min)

k_1 = rate constant of the pseudo-first order sorption (min^{-1})

k_2 = rate constant of the pseudo-second order sorption ($\text{g mg}^{-1} \text{ min}^{-1}$)

The rate constants of the pseudo-first order and the pseudo-second order (k_1 and k_2) can be obtained from the linear plot of $\log (q_e - q_t)$ and $\frac{t}{q_t}$ against t , respectively for different sorbent amount. The results are presented in Figure 4.11-4.12 and Table 4.4.

The kinetic parameters (Table 4.4) were calculated by using the linear equation obtained from the linear plot of experimental data using the pseudo-first order relation (eq. 4.3) and pseudo-second order relation (eq. 4.4), respectively. It can be seen that the correlation coefficients of pseudo-first order model (R_1^2) are relatively low and in the range of 0.828 – 0.993. Moreover, $q_{e,cal}$, the adsorption capacity at equilibrium calculated by using the linear equation obtained from the linear plot of pseudo-first order do not correspond with adsorption capacity at equilibrium observed in the experiments ($q_{e,exp}$) in the every adsorbent doses. On the other hand, in the case of pseudo-second order model, it was found that the correlation coefficients of pseudo-second order model (R_2^2) were between 0.994 to 1.000 and the $q_{e,cal}$ values also agreed very well with the $q_{e,exp}$ values, indicating a good fit of the kinetics model with the experimental data. Therefore, the sorption kinetics of Hg(II) and Ag(I) onto the AEPE-hectorite followed the pseudo-second order model. By this model, it is assumed that

(i) the adsorption occurred via chemisorptions which the adsorption behaviors may involve the complexation by sharing of electrons between metal cation and active sites on the adsorbent [56-58], (ii) the sorption followed a monolayer regime on the adsorbent surface and (iii) the rate of adsorption occurred rapidly at the initial step of adsorption [59]. In addition, the rate constant of the pseudo-second order (k_2) may be constant [65, 66] or increase [59], depending on the experimental set-up of the each system (e.g. temperature, adsorbent dose). In this research, k_2 increased in increasing adsorbent dose, therefore the adsorption equilibrium will be reached faster.

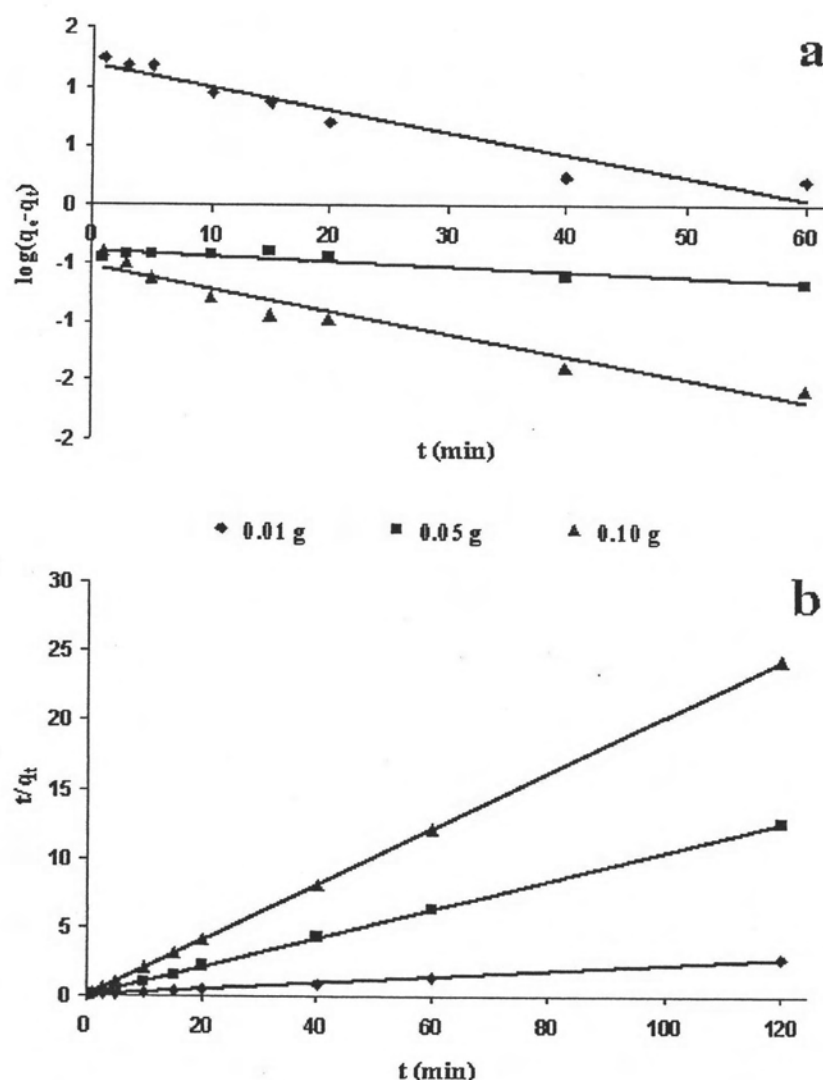


Figure 4.11 Pseudo-first order (a) and pseudo-second order (b) kinetics plot of the adsorption of Hg(II) ions onto the AEPE-hectorite.

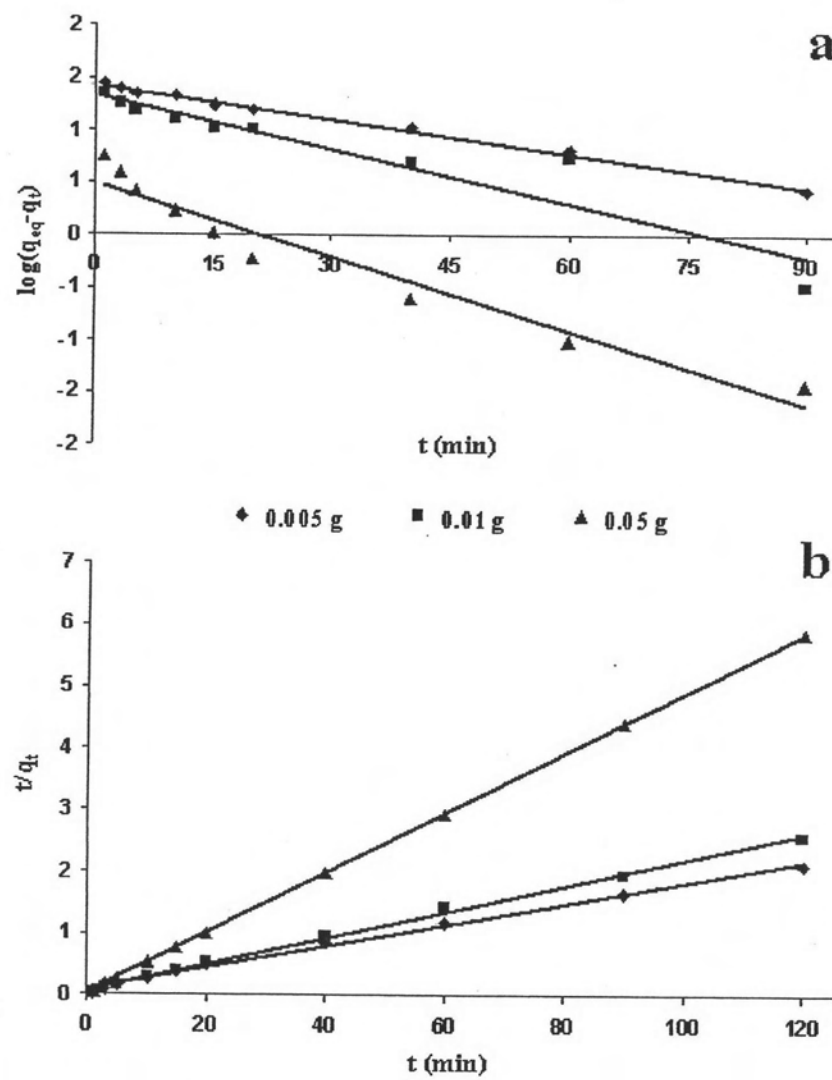


Figure 4.12 Pseudo-first order (a) and pseudo-second order (b) kinetics plot of the adsorption of Ag(I) ions onto the AEPE-hectorite.

Table 4.4 The kinetics parameter and constants for adsorption of Hg(II) and Ag(I) ions by AEPE-hectorite

Metal	Adsorbent dose (g)	$q_{e,exp}$ ^a (mg g ⁻¹)	Pseudo-first order model			Pseudo-second order model		
			Linear equation	$q_{e,cal}$ ^b (mg g ⁻¹)	$k_1 \times 10^{-2}$ (min ⁻¹)	R^2 ^c	Linear equation	$q_{e,cal}$ ^b (mg g ⁻¹)
Hg(II)	0.01	43.39	$Y = -0.019x + 1.188$	15.42	4.38	0.926	$Y = 0.0227x + 0.0545$	44.05
	0.05	9.57	$Y = -0.0045x - 0.3872$	0.41	1.04	0.828	$Y = 0.1046x + 0.0511$	9.56
	0.10	4.94	$Y = -0.019x - 0.5241$	0.30	4.44	0.933	$Y = 0.2023x + 0.0626$	4.94
Ag(I)	0.005	56.66	$Y = -0.0108x + 1.4239$	26.54	2.49	0.993	$Y = 0.0174x + 0.0915$	57.47
	0.01	46.64	$Y = -0.0171x + 1.3292$	21.34	3.94	0.886	$Y = 0.0211x + 0.0784$	47.39
	0.05	20.55	$Y = -0.0236x + 0.4973$	3.14	5.44	0.941	$Y = 0.0484x + 0.035$	20.66

^a The sorption capacity obtained by the experiments

^b The sorption capacity obtained by the calculation using linear equation

^c The correlation coefficients of pseudo-first order model

^d The correlation coefficients of pseudo-second order model

4.2.4 Effect of ionic strength (μ)

In natural water (e.g. fresh water or sea water), it contains ions other than metal ions of interest in different concentrations depending on the source. These ions may affect the adsorption efficiency of the AEPE-hectorite. For this reason, the effect of ionic strength was investigated by using NaNO_3 0.01 – 2.0 M and the results are shown in Table 4.5.

Table 4.5 Effect of ionic strength of solution on adsorption of Hg(II) and Ag(I) ions onto AEPE-hectorite

Concentration of NaNO_3 (M)	Times		Adsorption capacity (mg g ⁻¹) ^a	
	$\text{NaNO}_3:\text{Hg(II)}$	$\text{NaNO}_3:\text{Ag(I)}$	Hg(II)	Ag(I)
0.01	40	15	24.29 ± 0.19	30.71 ± 0.30
0.05	200	77	24.04 ± 0.26	31.71 ± 0.27
0.10	400	154	23.84 ± 0.19	32.10 ± 0.35
0.25	1000	385	23.25 ± 0.06	31.09 ± 0.12
0.50	2000	770	23.06 ± 0.12	30.96 ± 0.48
1.00	4000	1540	22.67 ± 0.02	31.53 ± 0.20
1.50	6000	2311	23.50 ± 0.10	30.93 ± 0.17
2.00	8000	3082	22.77 ± 0.09	30.36 ± 0.35

^a Mean \pm S.D. (n = 3)

A slight decrease of the adsorption capacity was observed from 24.29 to 22.67 mg g⁻¹ for Hg(II) when increased the concentration of NaNO_3 from 40 to 8000 time higher than Hg(II) concentration. This effect could be explained that Na^+ ions can interact well with the charged surface. Therefore, when increased NaNO_3 concentration in bulk solution, the competitive adsorption on the charged surface

between Na^+ and metallic species (i.e. Hg(OH)_2 and Ag^+) may occur resulting in a decrease in adsorption capacity. Nevertheless, in the case of Ag^+ ions, which are also high valency, an increase in ionic strength or NaNO_3 concentration do not affect the adsorption capacity. The results show non-specific trend when increased NaNO_3 concentration. However, the slight change in adsorption capacity of AEPE-hectorite observed when increased dramatically the ionic strength indicated that the adsorption behavior of AEPE-hectorite is independent to the ionic strength [14, 32, 60]. These results reveal that the adsorption process of the adsorbent occurred mainly via coordination with AEPE rather than ion exchange of metal ions onto the charged surface of AEPE-hectorite.

4.2.5 Effect of interfering ions

The ions other than Hg(II) and Ag(I) ions can be certainly found in natural water and wastewater and these cations may affect the adsorption of Hg(II) and Ag(I) ions by the adsorbents due to the competition with the analyte metal ions for the binding sites. Moreover, the anions can form complex with the analyte metal ions from insoluble compounds (i.e. precipitation). Thus, the effect of interfering ions such as cations, anions and other heavy metal ions were investigated to evaluate the selectivity of AEPE-hectorite towards Hg(II) and Ag(I) ions.

Cations

The cations (Na^+ , K^+ , Mg^{2+} and Ca^{2+}) of nitrate salts, were added separately to solutions with concentration of 0.5 and 2.0 M for Hg(II) solutions and 0.1 and 1.0 M for Ag(I) solutions. The adsorption efficiency of AEPE-hectorite for the metal ions of interest was determined. The results are shown in Table 4.6.

Table 4.6 Effect of cations on the adsorption of Hg(II) and Ag(I) ions by AEPE-hectorite

Salts	Concentration of salt (M)	Hg(II) ^a	Ag(I) ^a	
		Adsorption capacity (mg g ⁻¹) ^b	Concentration of salt (M)	Adsorption capacity (mg g ⁻¹) ^b
NaNO_3	0.5	22.98 ± 0.16	0.1	31.47 ± 0.33
	2.0	22.35 ± 0.30	1.0	31.59 ± 0.06
KNO_3	0.5	23.71 ± 0.26	0.1	30.20 ± 0.19
	2.0	22.60 ± 0.14	1.0	31.15 ± 0.49
$\text{Mg}(\text{NO}_3)_2$	0.5	22.54 ± 0.08	0.1	30.13 ± 0.26
	2.0	20.74 ± 0.42	1.0	29.71 ± 0.25
$\text{Ca}(\text{NO}_3)_2$	0.5	22.37 ± 0.28	0.1	29.26 ± 0.02
	2.0	21.63 ± 0.22	1.0	27.96 ± 0.36

^aThe concentration of Hg(II) and Ag(I) ions were 0.25 and 0.65 mM, respectively.

^b Mean \pm S.D. (n = 3)

It can be seen that there was no change in adsorption capacity of both metal ions in the presence of alkali metal ions (Na^+ and K^+) and the trend of the adsorption capacity is in accordance with the effect of ionic strength. The effect resulted from ionic strength in the presence of alkali metal ions do not occur at these concentrations but at higher concentration as reported previously in this work and by J.L.Gardea-Torresdey et.al [28]. On the other hand, a slight decrease in adsorption capacity was observed when the concentration of interfering alkali earth cations increased for two analytes metal ions. This reduction is due to the high valency of the alkali earth metal ions compared to alkali metal ions, Ag(I) and Hg(OH)_2 [11] and/or high ionic strength of background electrolyte solution containing alkali earth cations [61]. As a result, there could be the competition between the analyte metal ions and the interfering ions

of alkali earth metal ions for available sorption sites on the charged surface of AEPE-hectorite causing a reduction in uptake of Hg(II) and Ag(I) at the concentration of the alkali earth metal ions of 2.0 and 1.0 M, respectively. However, when comparing between the very high concentration of electrolyte salts and the slight decreasing of the sorption capacity, the ionic strength and interfering cations have little effect on adsorption efficiency. These results confirmed that the main sorption mechanism of Hg(II) and Ag(I) onto the AEPE-hectorite is the complex formation between AEPE and the analytes metal ions according to the Pearson's theory rather than ion exchange onto charged surface of the AEPE-hectorite. Moreover, the complex formation between the interfering cation and the ligand on the AEPE-hectorite could hardly occur according to the hard/soft – acid/base principle [51].

Anions

The effect of anions (NO_3^- , SO_4^{2-} and Cl^-) of sodium salts on adsorption of Hg(II) and Ag(I) was investigated. The results are listed in Table 4.7. It is clearly seen that NO_3^- and SO_4^{2-} did not affect the extraction of the two metal ions, except the case of Na_2SO_4 1.0 M for Ag(I) extraction. A decrease in extraction efficiency was observed and the reason for this is not clear yet. Furthermore, the presence of Cl^- led to the complex formation between Ag(I) and Cl^- resulting in the precipitation of AgCl in the solution [62] and obviously reduced the sorption capacity for Hg(II). It could be explained that Cl^- (0.5 and 2.0 M) in Hg(II) solution might form complex with Hg(II), giving different Hg-Cl species according to the formation constants listed in Table 4.8. Furthermore, the dominant species of Hg-Cl in solution containing 0.5 and 2.0 M NaCl solution are only HgCl_4^{2-} . These results showed that the adsorption of Hg-Cl complexes onto the AEPE-hectorite is less favorable than the Hg^{2+} , Hg(OH)^+ and Hg(OH)_2 , leading to a reduction of adsorption capacity in this case.

Table 4.7 Effect of anions on the adsorption of Hg(II) and Ag(I) ions by AEPE-hectorite

Salts	Concentration of salt (M)	Hg(II) ^a	Ag(I) ^a	
		Adsorption capacity (mg g ⁻¹) ^b	Concentration of salt (M)	Adsorption capacity (mg g ⁻¹) ^b
NaNO_3	0.5	22.98 ± 0.16	0.1	31.47 ± 0.33
	2.0	22.35 ± 0.30	1.0	31.59 ± 0.06
Na_2SO_4	0.5	22.63 ± 0.06	0.1	29.05 ± 0.07
	2.0	22.79 ± 0.26	1.0	23.57 ± 0.28
NaCl	0.5	14.59 ± 0.10	0.1	- ^c
	2.0	6.65 ± 0.20	1.0	- ^c

^aThe concentration of Hg(II) and Ag(I) ions were 0.25 and 0.65 mM, respectively.

^b Mean \pm S.D. ($n = 3$)

^c Silver precipitated as silver chloride.

Table 4.8 Aqueous speciation reaction and cumulative formation constants for mercury complexes with chloride ion ligand [63-64]

Reaction	Log K
$\text{Hg}^{2+} + \text{Cl}^- \rightleftharpoons \text{HgCl}^+$	6.74
$\text{Hg}^{2+} + 2\text{Cl}^- \rightleftharpoons \text{HgCl}_2$	13.22
$\text{Hg}^{2+} + 3\text{Cl}^- \rightleftharpoons \text{HgCl}_3^-$	14.07
$\text{HgCl}_3^- \rightleftharpoons \text{HgCl}_4^{2-}$	15.07
$\text{Hg}^{2+} + \text{Cl}^- + \text{H}_2\text{O} \rightleftharpoons \text{HgClOH} + \text{H}^+$	3.23

Heavy metal ions

The effect of heavy metal ions (Ni^{2+} , Cd^{2+} and Co^{2+}) on adsorption of Hg(II) and Ag(I) ions were studied by using concentrations equal to and ten times of that of Hg(II) and Ag(I) . The results are summarized in Table 4.9. It was found that the adsorption of Hg(II) onto the AEPE-hectorite was not affected by the presence of interfering heavy metal ions at the two concentrations. In case of Ag(I) , a slight decrease in adsorption capacity was observed in the presence of Ni^{2+} , Cd^{2+} and Co^{2+} . It is probably due to the competitive adsorption between Ag(I) and the all interfering heavy metal ions via ion exchange mechanism and/or complexation on the surface of AEPE-hectorite. The results indicated that the AEPE-hectorite had high affinity towards Hg(II) and Ag(I) ions.

Table 4.9 Effect of other heavy metal ions on the adsorption of Hg(II) and Ag(I) ions by AEPE-hectorite

Salts	Concentration (mM)	Hg(II) ^a	Ag(I) ^a	
		Adsorption capacity (mg g ⁻¹) ^b	Concentration (mM)	Adsorption capacity (mg g ⁻¹) ^b
NaNO_3	0.5×10^3	23.01 ± 0.25	0.1×10^3	31.73 ± 0.47
$\text{Ni}(\text{NO}_3)_2$	0.25	22.79 ± 0.22	0.65	30.41 ± 0.16
	2.50	23.29 ± 0.07	6.50	29.22 ± 0.29
$\text{Cd}(\text{NO}_3)_2$	0.25	22.93 ± 0.06	0.65	27.47 ± 0.29
	2.50	23.03 ± 0.07	6.50	26.42 ± 0.16
$\text{Co}(\text{NO}_3)_2$	0.25	22.72 ± 0.19	0.65	29.97 ± 0.20
	2.50	22.33 ± 0.13	6.50	28.31 ± 0.27

^aThe concentration of Hg(II) and Ag(I) ions were 0.25 and 0.65 mM, respectively.

^b Mean \pm S.D. ($n = 3$)

4.2.6 Adsorption isotherms

The adsorption equilibrium between metal ions in aqueous solution and the adsorbent (liquid / solid interface) can be described by adsorption isotherms. Langmuir and Freundlich relations are the two models commonly used in the study of the adsorption behavior. The Langmuir sorption isotherm is widely used to describe monolayer sorption, that is when the adsorption takes place at specific homogeneous sites within the adsorbent and no further adsorption can take place at that sites. For this reason, the adsorption capacity of the adsorbent is limited for the analytes. The Langmuir isotherm equation is shown in equation (4.5) [58, 65].

$$\frac{C_e}{q} = \frac{1}{bq_m} + \frac{C_e}{q_m} \quad (4.5)$$

where C_e = equilibrium concentration of the analyte in aqueous solution
 $(\text{mg L}^{-1} \text{ or mol L}^{-1})$

q = adsorption capacity of sorbent (mg g^{-1} or mol g^{-1})

q_m = maximum adsorption capacity of sorbent (mg g^{-1} or mol g^{-1})

b = Langmuir constant related to the affinity of binding sites
 $(\text{L mg}^{-1} \text{ or L mol}^{-1})$

The value of q_m and b are obtained by the linear plot of $\frac{C_e}{q}$ against C_e .

Furthermore, the essential features of Langmuir isotherm can be displayed in terms of dimensionless constant separation factor or equilibrium parameter, R_L , given by [57, 66]:

$$R_L = \frac{1}{1 + bC_i} \quad (4.6)$$

where b = Langmuir constant related to the affinity of binding sites
 $(\text{L mg}^{-1} \text{ or L mol}^{-1})$

C_i = initial concentration of metal ions in aqueous solution
 $(\text{mg L}^{-1} \text{ or mol L}^{-1})$

The parameter R_L indicates the type of isotherm as presented in Table 4.10.

Table 4.10 The mean of R_L value that associates with the type of isotherm

Value of R_L	Type of isotherm
$R_L > 1$	Unfavorable
$R_L = 1$	Linear
$0 < R_L < 1$	Favorable
$R_L = 0$	Irreversible

The Freundlich isotherm is an empirical model based on sorption on heterogeneous surface or surface supporting sites of various affinities. The isotherm is presented by the following equation [57-58].

$$\log q = \log K_f + \frac{1}{n} \log C_e \quad (4.7)$$

where K_f = Freundlich constant related to adsorption capacity
 $(\text{mg g}^{-1} \text{ or mol g}^{-1})$

n = Freundlich constant related to adsorption intensity

K_f and n can be determined from linear plot of $\log q$ against $\log C_e$.

In this study, the solution of concentration $30\text{-}500 \text{ mg L}^{-1}$, having initial pH of 3.0 were used in adsorption experiments at temperature $25.0 \pm 0.5^\circ\text{C}$. The results show

that the sorption capacity of the two metal ions increased rapidly at low initial concentrations (Figure 4.13). And then, the experimental data of adsorption of Hg(II) and Ag(I) were taken for linear plotting using Langmuir and Freundlich models (Figure 4.14 and 4.15). The obtained linear equations gained by curve fitting were listed in Table 4.11 and 4.12. The Langmuir and Freundlich parameters were also calculated.

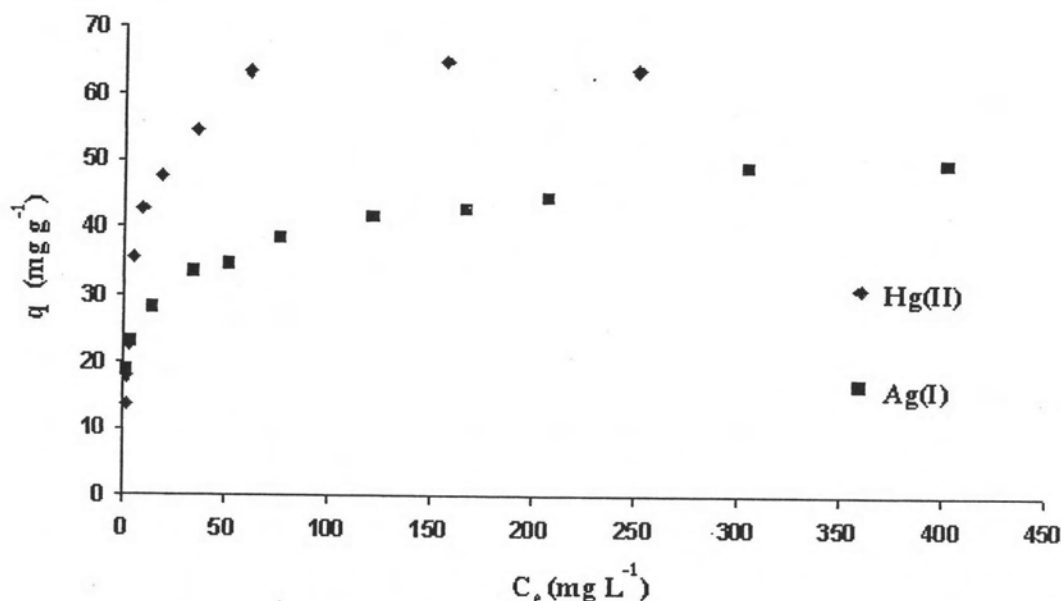


Figure 4.13 Adsorption isotherms of Hg(II) and Ag(I) ions.

The results shown in Table 4.11 and 4.12 with the correlation coefficient (R^2) indicates that adsorption isotherm of Ag(I) fit the Langmuir and Freundlich models ($R^2 \geq 0.99$), while the adsorption isotherm of Hg(II) fit the Langmuir model better than Freundlich model.

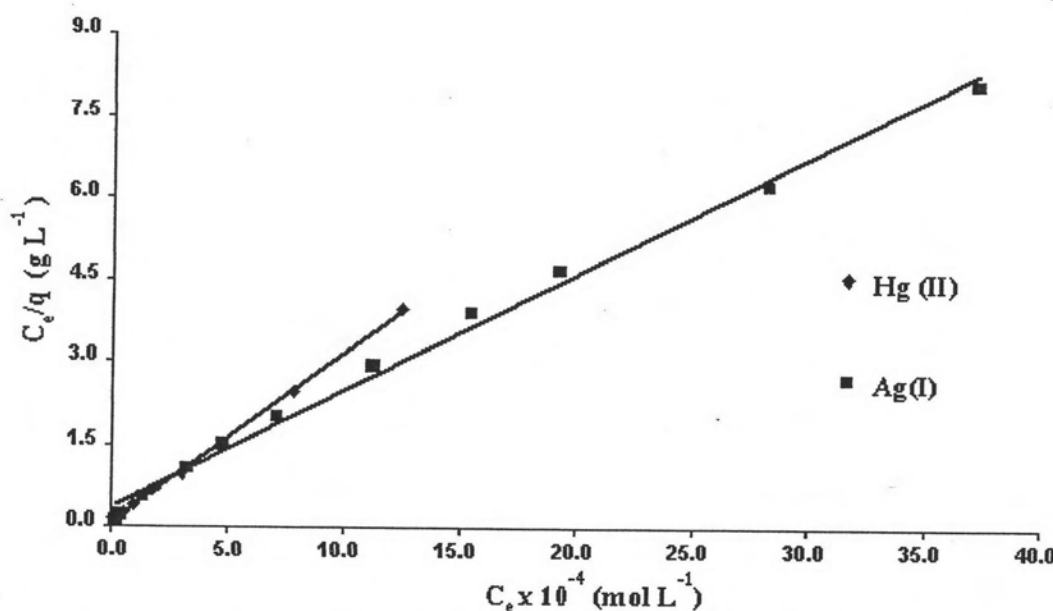


Figure 4.14 Langmuir isotherm plots of adsorption of Hg(II) and Ag(I) ions onto the AEPE-hectorite at $25.0 \pm 0.5^\circ\text{C}$.

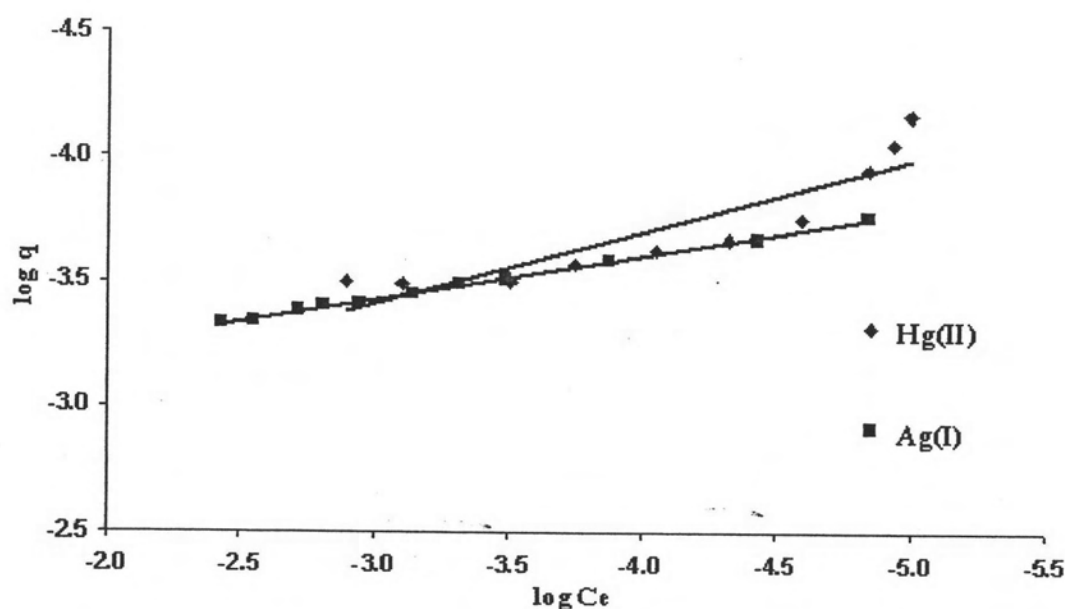


Figure 4.15 Freundlich isotherm plots of adsorption of Hg(II) and Ag(I) ions onto the AEPE-hectorite at $25.0 \pm 0.5^\circ\text{C}$.

Table 4.11 The Langmuir isotherm parameters at $25.0 \pm 0.5^\circ\text{C}$

Metal	Linear equation	R^2	$b \times 10^4$ (L mol ⁻¹)	$q_{m,cal} \times 10^{-4}$ (mol g ⁻¹) ^a	$q_{m,cal}$ (mg g ⁻¹) ^a	$q_{m,exp}$ (mg g ⁻¹) ^b	R_L
Hg(II)	$Y = 3061x + 0.0837$	0.999	3.66	3.27	65.53	63.99	0.014 - 0.159
Ag(I)	$Y = 2134.9x + 0.3288$	0.994	0.65	4.68	50.53	49.47	0.032 - 0.298

^a The maximum sorption capacity obtained by the calculation.

^b The maximum sorption capacity obtained by the experimental.

Table 4.12 The Freundlich isotherm parameters at $25.0 \pm 0.5^\circ\text{C}$

Metal	Linear equation	R^2	$K_f \times 10^{-3}$ (mol g ⁻¹)	K_f (mg g ⁻¹)	$1/n$	n
Hg(II)	$Y = 0.2927x - 2.5263$	0.817	2.74	548.67	0.2927	3.42
Ag(I)	$Y = 0.1749x - 2.9036$	0.997	1.25	134.68	0.1749	5.72

However, the adsorption behavior of AEPE-hectorite for Ag(I) and Hg(II) seem to follow the Langmuir model. It could be confirmed by using the evidences as followings : (i) The Langmuir constants (b) obtained are high for adsorption of each metal ion onto the adsorbent. It indicates that the sorption mechanism of metal ions onto AEPE-hectorite are coordination of metal ions with donor sites of the ligand (sulfur and nitrogen donor atom) [67], (ii) the maximum sorption capacity (q_m) of both Hg(II) and Ag(I) from the experiments correspond to the q_m from the calculation of Langmuir model and reach a saturation of the sorption capacity as shown in Figure 4.13 indicating the monolayer coverage and no further adsorption could occur and (iii) The calculated R_L values are between 0.014 to 0.298, in the range of $0 < R_L < 1$, which indicate that the adsorption of Hg(II) and Ag(I) onto the AEPE-hectorite are favorable [58]. By the results corresponding to Langmuir relation, it could be assumed that the adsorption mechanisms of Hg(II) and Ag(I) on the AEPE-hectorite are the chemisorption via coordination of the AEPE ligand on the hectorite with the metal ions and the monolayer coverage of metal ions on the AEPE-hectorite surface occurred [57, 68]. Furthermore, the adsorption behavior of the two metal ions on the APEE-hectorite surface was confirmed by the good fitting of the results to the pseudo-second order kinetics, which has assumptions based on monolayer adsorption and chemisorption.

In addition, the ion exchange process could also occur in the case of Ag(I) because the dominant Ag(I) species are Ag^+ cation at the pH of extraction that can interact with charged surface of AEPE-hectorite. On the other hand, the dominant Hg(II) species are Hg(OH)_2 which would not adsorb onto the surface of AEPE-hectorite via electrostatic interaction. Moreover, the experimental results of adsorption of Ag(I) could fit to Freundlich model ($R^2 = 0.997$) indicating that the adsorption occurred on heterogeneous surface or supporting sites of various affinity [69]. These active sites possibly correspond to ion exchangeable sites on clay surface and complexing sites of the ligand on surface.

Finally, the results let conclude that the adsorption isotherm of Hg(II) and Ag(I) onto the AEPE-hectorite can be describe by Langmuir's model and the maximum adsorption capacity of Hg(II) and Ag(I) onto the AEPE-hectorite are 0.33 and 0.47 mmol g⁻¹, respectively. It was observed that the adsorption capacity of Ag(I) is higher than Hg(II) probably due to the combination of the ion exchange and coordination mechanism for Ag(I) onto the AEPE-hectorite.

Table 4.13 The maximum adsorption capacity of the other modified materials for mercury(II) ions removal

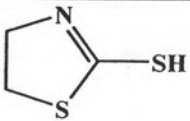
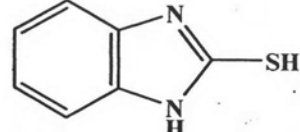
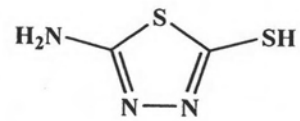
Solid support	Chelating ligand	q_m (mmol g ⁻¹)	Ref.
Hexagonal mesoporous Silica	 2-Mercaptothiazoline	2.34	[37]
Silica	 2-Mercaptobenzimidazole	1.35	[70]
	 5-Amino-1,3,4-thiadiazole-2-thiol	0.49	[71]

Table 4.13 The maximum adsorption capacity of the other modified materials for mercury(II) ions removal (continued)

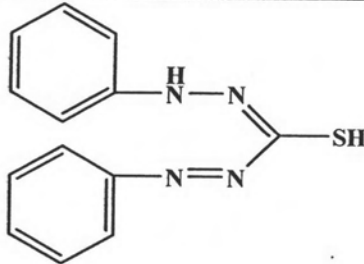
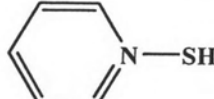
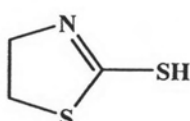
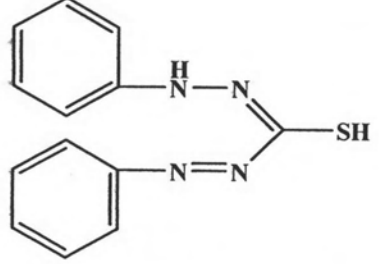
Solid support	Chelating ligand	q_m (mmol g ⁻¹)	Ref.
Silica	 1,5-Diphenylthiocarbazone	0.32	[72]
MCM-41	 2-Mercaptopyridine	0.14	[73]
Poly(EGDMA-HEMA) microbead	 2-Mercaptothiazoline	0.09	[74]
	 1,5-Diphenylthiocarbazone	0.25	[75]
		0.21	[24]

Table 4.13 The maximum adsorption capacity of the other modified materials for mercury(II) ions removal (continued)

Solid support	Chelating ligand	q_m (mmol g ⁻¹)	Ref.
Fluorohectorite clay		0.74	[38]
	3-Mercaptopropyltrimethoxysilane		
Montmorillonite		2.09	[76]
	1,3,4-Thiadiazole-2,5-dithiol		
		0.33	[10]
	3-Mercaptopropyltrimethoxysilane		
Hectorite		0.33	This work
	2-(3-(2-Aminoethylthio)propylthio) ethanamine (AEPE)		

When comparing the adsorption capacity of modified hectorite to other materials reported by other authors (Table 4.13), the adsorbent prepared in this work has fairly good capacity for Hg(II) ions. In case of Ag(I), the adsorption capacity of our the adsorbent could not be compared to other materials because we could not find any papers of other adsorbent.

4.3 Application to real water samples

Finally, the AEPE-hectorite was applied to remove Hg(II) and Ag(I) ions in real water samples. In this work, the waste water from the laboratory of the gem and jewelry institute of Thailand and the sea water at Layong province were collected and used in the experiment of Ag(I) and Hg(II), respectively.

The sea water

The sea water was filtered and the pH of sample solution was measured. The concentration of Hg(II) ions in the sea water was analyzed before used in extraction experiments. It was found that the pH of the sea water was 8.2 and the concentration of Hg(II) ions was very low and could not be detected by CVAAS.

Thus, the standard Hg(II) solution was added to the seawater and the pH and the concentration of Hg(II) ion were about 8.0 and 50 mg L^{-1} , respectively. The experiments were carried out using 0.01, 0.02 and 0.04 g of the AEPE-hectorite with the extraction time of 60 min. The results were presented in Figure 4.16. It was found that the best removal efficiency for Hg(II) ions in the sea water is 96.43% by using the AEPE-hectorite 0.04 g and 0.01 g of AEPE-hectorite could only remove Hg(II) ions about 57.64 % or 14.04 mg g^{-1} in the adsorption capacity term, which was much lower than the maximum adsorption capacity (65.53 mg g^{-1}). This result could be attributed to the effect of chloride ions in the sea water that can form complexes with Hg(II). The results are in agreement with the interfering anions results reported previously.

The wastewater from the laboratory of Gem and Jewelry Institute of Thailand

This wastewater had a very low pH (pH 1.0) and a high concentration of silver (about 6,600 mg L⁻¹). This wastewater must be diluted to obtain a wastewater solution which had the pH and the concentration of silver about pH 1.5 and 60 mg L⁻¹, respectively. The extraction experiments were performed by using 0.01, 0.02 and 0.03 g of AEPE-hectorite and the contact time of 60 min.

The results show that the removal efficiency increased from 48.29 to 95.03 % with the increasing of the AEPE-hectorite dose (Figure 4.16). It indicates that the AEPE-hectorite can be used to extract silver in solution having low pH. This is probably due to the presence of the sulfur donor atom of the AEPE ligand on the hectorite.

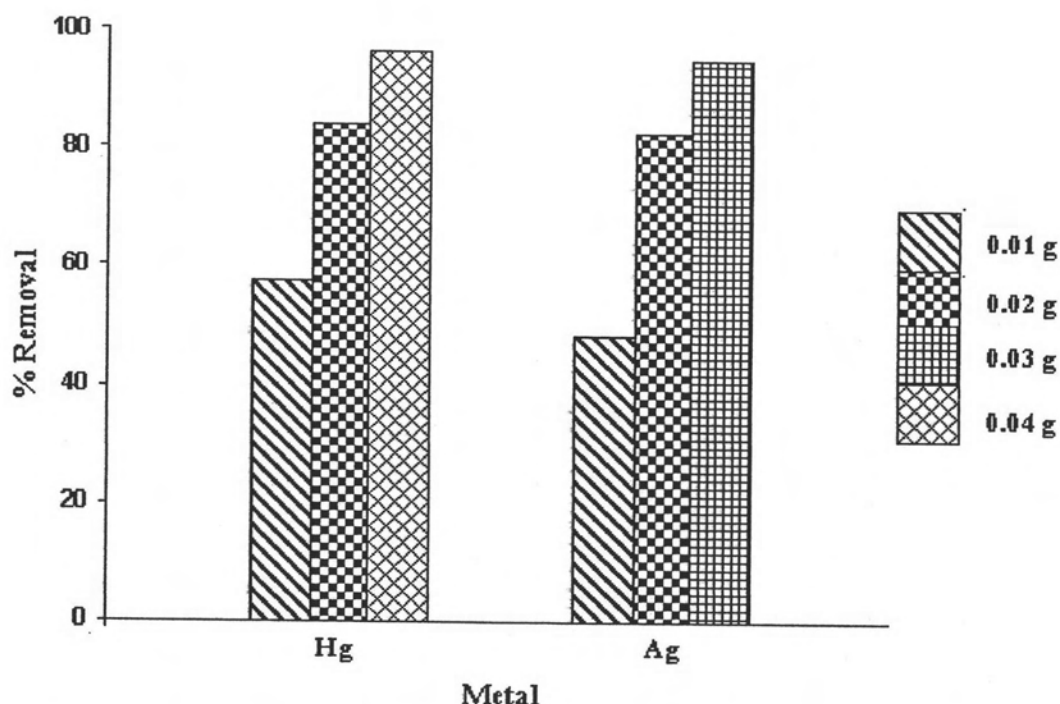


Figure 4.16 The removal efficiency of Hg(II) and Ag(I) ions in the real water sample by AEPE-hectorite.

These results confirm that the AEPE-hectorite can be applied to remove the Hg(II) and Ag(I) ions in the real water samples although the real water samples have low pH and/or high concentration of the matrix.